Journal of Biomolecular NMR, 5 (1995) 82–86
ESCOM

J-Bio NMR 236

# Sequential backbone assignment of uniformly $^{13}C$-labeled RNAs by a two-dimensional P(CC)H-TOCSY triple resonance NMR experiment

S.S. Wijmenga[a,*], H.A. Heus[b], H.A.E. Leeuw[b], H. Hoppe[b], M. van der Graaf[b] and C.W. Hilbers[a,b]

[a]*SON/NWO National HF-NMR Facility and* [b]*Laboratory of Biophysical Chemistry, Toernooiveld, NL-6525 ED Nijmegen, The Netherlands*

Received 25 July 1994
Accepted 11 October 1994

*Keywords:* Labeled RNA; Triple resonance; HeteroTOCSY; Assignment

**Summary**

A new $^{1}H$-$^{13}C$-$^{31}P$ triple resonance experiment is described which allows unambiguous sequential backbone assignment in $^{13}C$-labeled oligonucleotides via through-bond coherence transfer from $^{31}P$ via $^{13}C$ to $^{1}H$. The approach employs INEPT to transfer coherence from $^{31}P$ to $^{13}C$ and homonuclear TOCSY to transfer the $^{13}C$ coherence through the ribose ring, followed by $^{13}C$ to $^{1}H$ J-cross-polarisation. The efficiencies of the various possible transfer pathways are discussed. The most efficient route involves transfer of $^{31}P_i$ coherence via $C4'_i$ and $C4'_{i-1}$, because of the relatively large $J_{PC4'}$ couplings involved. Via the homonuclear and heteronuclear mixing periods, the $C4'_i$ and $C4'_{i-1}$ coherences are subsequently transferred to, amongst others, $H1'_i$ and $H1'_{i-1}$, respectively, leading to a 2D $^{1}H$-$^{31}P$ spectrum which allows a sequential assignment in the $^{31}P$-$^{1}H1'$ region of the spectrum, i.e. in the region where the proton resonances overlap least. The experiment is demonstrated on a $^{13}C$-labeled RNA hairpin with the sequence 5'(GGGC-CAAA-GCCU)3'.

The first crucial step in NMR structural studies involves the unambiguous assignment of resonances. Traditionally, sequential assignment of nucleic acids has been based on through-space NOE interactions (Wüthrich, 1986; Mooren et al., 1991; Wijmenga et al., 1993,1994c), which suffer from the inability to unambiguously distinguish inter- and intraresidue interactions. Through-bond interactions do not have this drawback. The development by Bax and co-workers (Ikura et al., 1990,1991; Kay et al. 1990,1991; Bax and Ikura, 1991; Powers et al., 1991; Grzesiek and Bax, 1992) of sequential assignment techniques based on through-bond coherence transfer using multi-dimensional triple resonance NMR experiments has revolutionized the field of solution structure determination of isotopically labeled proteins (see e.g. Clore and Gronenborn, 1990,1991). With the recent advent of biochemical enrichment techniques for RNAs (Simon et al., 1990; Batey et al., 1993; Nikonowicz et al., 1992; Michnicka et al., 1993; Wijmenga et al., 1994a), these NMR techniques can now be modified and applied to nucleic acids as well. Already a number of NMR experiments have been reported that apply through-bond coherence transfer to correlate (i) base and sugar protons (Sklenář et al., 1993a,b; Farmer II et al., 1993,1994); (ii) the H2 and H8 protons within the adenine base (Legault et al., 1994; Marino et al., 1994; Wijmenga et al., 1994b); and to achieve (iii) sequential assignment via the sugar–phosphate backbone, for which we developed a 3D $^{1}H$-$^{13}C$-$^{31}P$ triple resonance experiment, HCP (Heus et al., 1994; Wijmenga et al., 1994a). The 3D HCP experiment allows sequential assignment, since at each $C4'_i$ frequency a cross peak is found at ($H4'_i$, $P_i$), where $P_i$ is the P5' atom of residue i, and at ($H4'_i$, $P_{i+1}$), where $P_i$ is the P3' atom of residue i+1. To establish the 5'→3' direction the cross peaks at the $C5'_i$ frequency are used, since $C5'_i$ only correlates with $P_i$ (P5' of residue i) and not with $P_{i+1}$ (P3' of residue i). To complete the assignment, the desired connection between $C4'_i$ and $C5'_i$ is established via a 2D CCH-TOCSY experiment or HCCH-TOCSY (Nikonowicz and Pardi, 1993). The CCH-TOCSY correlates the $^{13}C$ reson-

*To whom correspondence should be addressed.

ances with the $^1$H resonances of the sugar ring via a C→C mixing sequence, followed by a C→H cross-polarisation, both using DIPSI3 (Shaka et al., 1988) (for C→H transfer, cross-polarisation is a more sensitive technique than refocussed INEPT (Zuiderweg, 1990)). The correlation can be found most conveniently from the $^{13}$C-TOCSY ladders at the H1' frequencies, since the H1' resonances overlap least. We demonstrated the assignment procedure on a $^{13}$C-labeled RNA hairpin with the sequence 5'(GGGC-CAAA-GCCU)3', and showed that a complete sequential walk could be obtained (Heus et al., 1994). In order to take advantage of the higher resolution of the H1' region, we present here a new NMR experiment, termed P(CC)H-TOCSY, for sequential backbone assignment of $^{13}$C-labeled RNAs. It combines the PCH and CCH-TOCSY experiments into one triple resonance NMR experiment and allows a sequential backbone assignment to be made via the H1' resonances in a 2D $^1$H-$^{31}$P spectrum.

The 2D P(CC)H-TOCSY pulse scheme used in this study is given in Fig. 1. The experiment is employed to transfer coherence from $^{31}$P to $^1$H1' through $^{13}$C, via the primary coherence transfer pathways sketched in Fig. 2. The pulse sequence starts with a series of 180° $^1$H pulses to saturate the $^1$H magnetisation and create NOE transfer to phosphorus, after which a $90^\circ_x$ pulse on $^{31}$P creates transverse $^{31}$P coherence ($P_y$). After the $^{31}$P evolution period ($t_1$), the in-phase $^{31}$P coherence, $P_y$, is transferred into antiphase coherence, $P_xC_z$, during the two delays $\tau$. The second $90^\circ_y$ $^{31}$P pulse converts this antiphase coherence into zz-order, $P_zC_z$. The gradient spoil pulse at this point removes all unwanted transverse coherence, after which antiphase $P_zC_x$ coherence is created by the first $90^\circ_y$ $^{13}$C pulse. During the delays $\tau'$, $P_zC_x$ is refocussed into in-phase $C_y$ coherence. After application of a $^{13}$C trim pulse along the y-axis to remove unwanted $^{13}$C coherence, the in-phase $C_y$ coherence is transferred through the network of J-coupled $^{13}$C spins of the sugar ring via a homonuclear $^{13}$C-$^{13}$C mixing sequence (DIPSI3). Finally, the $C_y$ coherence is transferred to its directly bonded $^1$H via cross-polarisation by applying a DIPSI3 mixing sequence on both $^{13}$C and $^1$H simultaneously, after which the $^1$H signal is acquired during $t_2$ with GARP (Shaka et al., 1985) decoupling of $^{13}$C.

Three main transfer pathways, schematically depicted in Fig. 2, are possible, namely (i) the C4'-routes (Fig. 2A) $P_i \rightarrow C4'_i \rightarrow C1'_i \rightarrow H1'_i$ and $P_i \rightarrow C4'_{i-1} \rightarrow C1'_{i-1} \rightarrow H1'_{i-1}$; (ii) the C3'-route (Fig. 2B) $P_i \rightarrow C3'_{i-1} \rightarrow C1'_{i-1} \rightarrow H1'_{i-1}$; and (iii) the C5'-route (Fig. 2B) $P_i \rightarrow C5'_i \rightarrow C1'_i \rightarrow H1'_i$. The transfer efficiency of each of these routes depends on the J-couplings involved. The most critical first step in each of the routes is the transfer from in-phase $P_y$ coherence into in-phase $C_y$ coherence. This will therefore be discussed in detail below. The efficiency of the conversion of in-phase $P_y$ coherence into antiphase $P_xC_z$ coherence is given by the following equations:

$$\mathrm{Tr}\ P_iC4'_i = \sin(2\pi J_{P_iC4'_i}\tau)\cos(2\pi J_{P_iC4'_{i-1}}\tau)\cos(2\pi J_{P_iC3'_{i-1}}\tau)\cos(2\pi J_{P_iC5'_i}\tau) \quad (1a)$$

$$\mathrm{Tr}\ P_iC4'_{i-1} = \sin(2\pi J_{P_iC4'_{i-1}}\tau)\cos(2\pi J_{P_iC4'_i}\tau)\cos(2\pi J_{P_iC3'_{i-1}}\tau)\cos(2\pi J_{P_iC5'_i}\tau) \quad (1b)$$

$$\mathrm{Tr}\ P_iC3'_{i-1} = \sin(2\pi J_{P_iC3'_{i-1}}\tau)\cos(2\pi J_{P_iC4'_{i-1}}\tau)\cos(2\pi J_{P_iC4'_i}\tau)\cos(2\pi J_{P_iC5'_i}\tau) \quad (2)$$

$$\mathrm{Tr}\ P_iC5'_i = \sin(2\pi J_{P_iC5'_i}\tau)\cos(2\pi J_{P_iC4'_{i-1}}\tau)\cos(2\pi J_{P_iC4'_i}\tau)\cos(2\pi J_{P_iC3'_{i-1}}\tau) \quad (3)$$

The most efficient transfer is from $P_i$ to $C4'_i$ and $C4'_{i-1}$, because of the rather large three-bond $J_{P_iC4'_i}$-couplings and $J_{P_iC4'_{i-1}}$-couplings involved. $J_{P_iC4'_i}$ and $J_{P_iC4'_{i-1}}$ depend on the

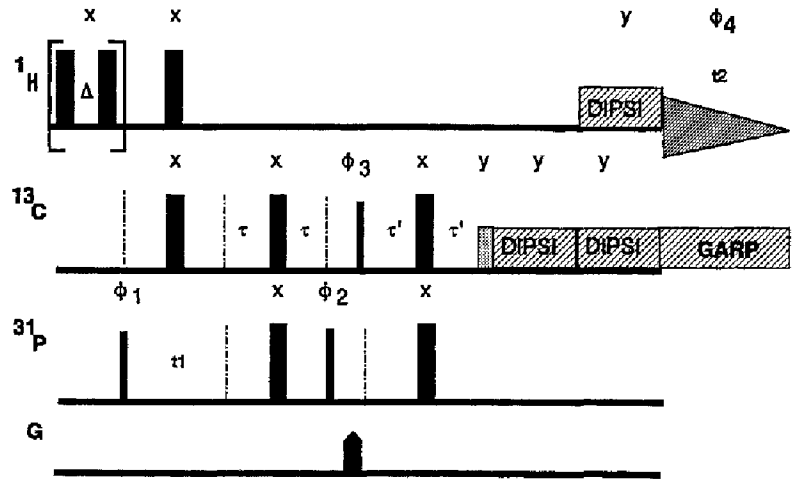


Fig. 1. Pulse sequence of the P(CC)H-TOCSY experiment. The thick and thin filled bars indicate 90° and 180° pulses, respectively. The dotted bar before the DIPSI sequence indicates a $^{13}$C trim pulse. Phase cycling was as follows: $\phi_1$ = x,x,–x,–x (with TPPI; Marion and Wüthrich, 1983); $\phi_2$ = y; $\phi_3$ = y,–y; $\phi_4$ = x,–x,–x,x. Details concerning delays are given in the legend of Fig. 4.

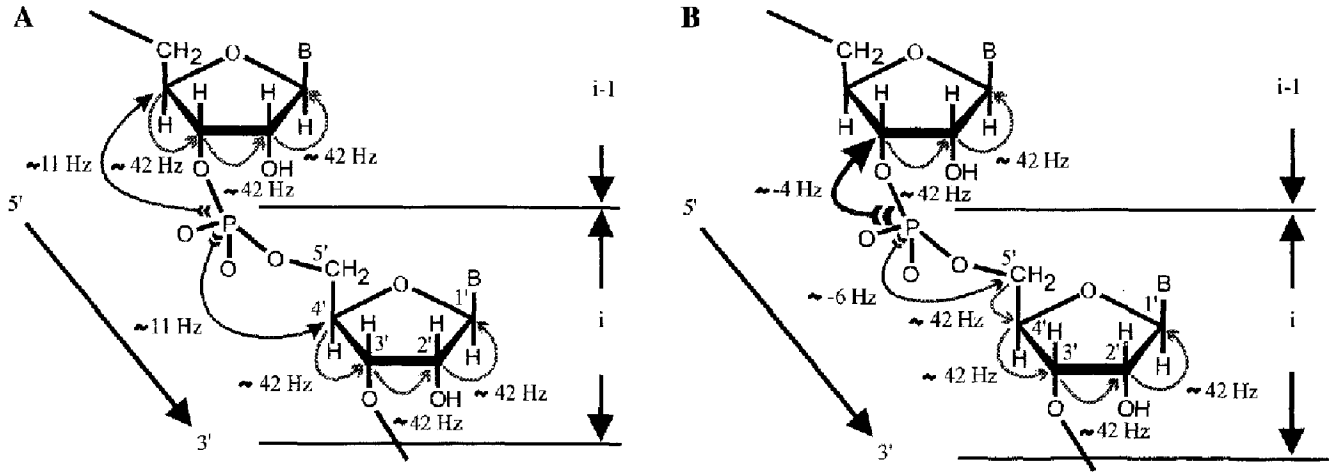


Fig. 2. Schematic of the RNA ribose–phosphate backbone, showing the coherence pathways in the P(CC)H-TOCSY experiment. (A) The main C4'-route (see text). (B) The C3'- and C5'-routes, as indicated by arrows (see text).

torsion angles ε and β, respectively. They are usually found in the trans range, resulting in a value of approximately 10 Hz for these J-couplings. The transfer from $P_i$ to $C3'_{i-1}$ and $C5'_i$ is less efficient, due to the smaller two-bond J-couplings involved, which are –4–5 and –5–6 Hz, respectively. Subsequent refocussing of antiphase $P_zC_x$ into in-phase $C_y$ coherence is governed by

$$\mathrm{Tr}\ C4'_iP_i = \sin(2\pi J_{P_iC4'_i}\tau')\cos(2\pi J_{P_{i+1}C4'_i}\tau')\cos(2\pi J_{CC}\tau')^2 \quad (4a)$$

$$\mathrm{Tr}\ C4'_{i-1}P_i = \sin(2\pi J_{P_iC4'_{i-1}}\tau')\cos(2\pi J_{P_{i-1}C4'_{i-1}}\tau')\cos(2\pi J_{CC}\tau')^2 \quad (4b)$$

$$\mathrm{Tr}\ C3'_{i-1}P_i = \sin(2\pi J_{P_iC3'_{i-1}}\tau')\cos(2\pi J_{CC}\tau')^2 \quad (5)$$

$$\mathrm{Tr}\ C5'_iP_i = \sin(2\pi J_{P_iC5'_i}\tau')\cos(2\pi J_{CC}\tau') \quad (6)$$

where $J_{CC}$ stands for the $^1$J-couplings between the $^{13}$C atoms of the sugar ring, which are of the order of 42 Hz. Again, the most efficient transfer is via C4'. The total transfer efficiency for the conversion of in-phase $P_y$ into in-phase $C_y$ coherence is the product of the transfer functions of the two individual steps:

$$\mathrm{Trt}\ P_iC4'_i = \mathrm{Tr}\ P_iC4'_i \times \mathrm{Tr}\ C4'_iP_i \quad (7a)$$

$$\mathrm{Trt}\ P_iC4'_{i-1} = \mathrm{Tr}\ P_iC4'_{i-1} \times \mathrm{Tr}\ C4'_{i-1}P_i \quad (7b)$$

$$\mathrm{Trt}\ P_iC3'_{i-1} = \mathrm{Tr}\ P_iC3'_{i-1} \times \mathrm{Tr}\ C3'_{i-1}P_i \quad (8)$$

$$\mathrm{Trt}\ P_iC5'_i = \mathrm{Tr}\ P_iC5'_i \times \mathrm{Tr}\ C5'_iP_i \quad (9)$$

As can be seen in Fig. 3, for all three routes the optimum efficiency is reached at $\tau = \tau' \approx 12.5$ ms. Destructive interference prohibits any effective transfer at longer delay times. Only at τ values of approximately 40–50 ms a second optimum occurs (outside the region shown). The

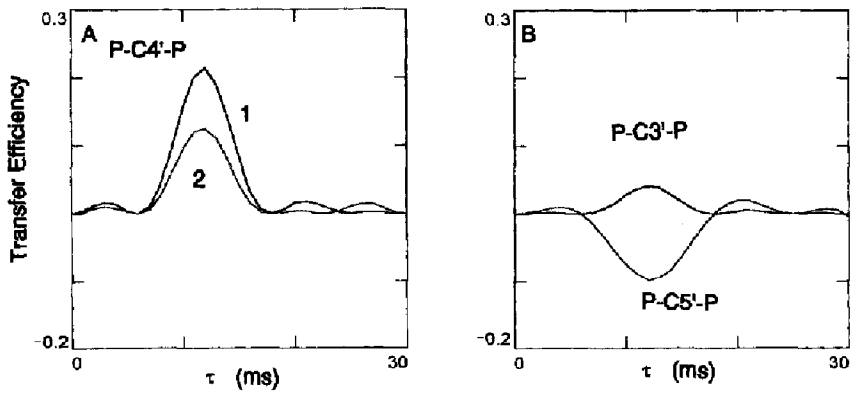


Fig. 3. Transfer efficiencies of the conversion of in-phase $P_y$ coherence into in-phase $C_x$ coherence in the P(CC)H-TOCSY experiment for the three primary pathways given in Fig. 2. (A) Transfer efficiency of the C4'-routes calculated for two sets of J-couplings: curve 1 with $JP_iC4'_i$ = 10 Hz, $JP_iC4'_{i-1}$ = 10 Hz, $JP_iC4'_{i+1}$ = 10 Hz, $JP_iC3'_{i-1}$ = 4 Hz, $JP_iC5'_i$ = 6 Hz, $J_{CC}$ = 42 Hz; curve 2: $JP_iC4'_i$ = 8 Hz, $JP_iC4'_{i-1}$ = 10 Hz, $JP_iC4'_{i+1}$ = 10 Hz, $JP_iC3'_{i-1}$ = 4 Hz, $JP_iC5'_i$ = 6 Hz, $J_{CC}$ = 42 Hz. (B) Transfer efficiencies of the C3'- and C5'-routes calculated with the following J-couplings: $JP_iC4'_i$ = 10 Hz, $JP_iC4'_{i-1}$ = 10 Hz, $JP_iC4'_{i+1}$ = 10 Hz, $JP_iC3'_{i-1}$ = 4 Hz, $JP_iC5'_i$ = 6 Hz, $J_{CC}$ = 42 Hz.

efficiency is considerably higher for the C4'-routes (Fig. 3A) than for the C3'- and C5'-routes (Fig. 3B). The C5'-route leads to in-phase $^{13}C$ coherence with negative sign, since the C5'-spin is J-coupled only to the C4'-spin, whereas C4' and C3' each have two J-coupling partners. Finally, the in-phase $C_y$ coherence is transferred through the J-coupled network of sugar $^{13}C$ atoms using a DIPSI3 mixing sequence. To obtain sufficient transfer to C1' a relatively long isotropic mixing time of 13 ms was used, while for the cross-polarisation a mixing time of 6.5 ms was chosen to obtain optimal transfer from $^{13}C$ to $^{1}H$ via the $^{1}J_{CH}$-couplings of approximately 150 Hz.

Thus, with this pulse sequence, coherence is transferred from $P_i$ to $H1'_i$ and to $H1'_{i-1}$ mainly via $C4'_i$ and $C4'_{i-1}$, respectively, as indicated in Fig. 2A. The alternate pathways via $C3'_i$ and $C5'_{i-1}$ (Fig. 2B) contribute, but less efficiently, to the $P_i$ to $H1'_i$ and $H1'_{i-1}$ correlations, respectively. The torsion angle dependence of the $P_i$ to $C4'_i$ and $C4'_{i-1}$ transfer efficiencies will be discussed in detail elsewhere. However, we note here one particular feature. Under certain circumstances the ε torsion may shift from its usual trans range to the $g^-$ range, leading to a decrease in $J_{P_iC4'_{i-1}}$ from approximately 10 Hz to approximately 3–4 Hz and resulting in a decreased efficiency of the $P_i$ to $C4'_{i-1}$ transfer. Simultaneously, however, the $^{3}J_{P_iC2'_{i-1}}$-coupling increases from a small value (≈ 1 Hz) for $\varepsilon^t$ to approximately 8 Hz for $\varepsilon^-$, resulting in coherence transfer from $P_i$ to $C2'_{i-1}$. This opens up an alternative pathway for $P_i$ to $H1'_{i-1}$ transfer, the C2'-route $P_i \rightarrow C2'_{i-1} \rightarrow C1'_{i-1} \rightarrow H1'_{i-1}$. The C2' → C1' transfer by isotropic mixing is quite efficient, since it requires only one $^{13}C$ transfer step. Thus, the $P_i \rightarrow H1'_{i-1}$ coherence transfer, which occurs mainly via $C4'_{i-1}$ when ε is in its usual trans range, is taken over by the C2'-route when ε flips to $g^-$, making the efficiency of the transfer of coherence from $P_i \rightarrow H1'_{i-1}$ effectively independent of the angle ε. Such an alternate route does not exist for $P_i$ to $H1'_i$ via $C4'_i$ when β shifts from its usual trans value.

The utility of the experiment is demonstrated on the uniformly $^{13}C$-labeled RNA 12-mer, which forms a hairpin structure in solution as schematically represented as an inset in Fig. 4. Figure 4 shows the $^{31}P/H1'$ region of

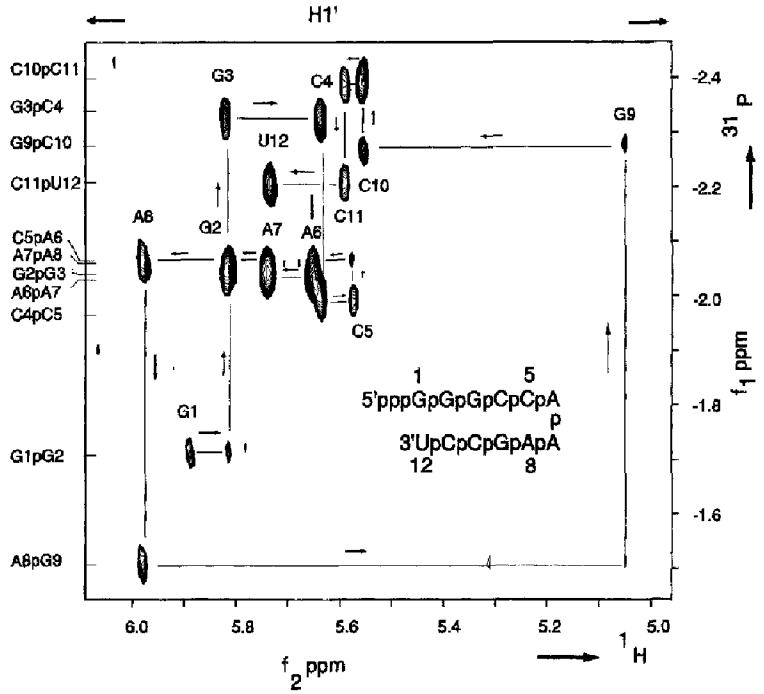


Fig. 4. H1' region of the 600 MHz 2D P(CC)H-TOCSY spectrum of a $^{13}C$-labeled RNA hairpin with a CAAA tetranucleotide loop, shown schematically in the inset, in $D_2O$ at 30 °C. The arrows indicate the 5' → 3' direction of the sequential walk along the sugar phosphate backbone. The labels at the cross peaks indicate the H1' assignment, while the $^{31}P$ assignment is given along the left side of the spectrum at the vertical position ($^{31}P$) of the cross peaks. The chemical shifts are referenced relative to TSP for the $^{1}H$ and $^{31}P$ dimensions; for $^{31}P$ the 0 ppm chemical shift value is obtained by multiplying the $^{1}H$ TSP frequency by 0.40480793, which corresponds to calibration relative to inorganic phosphate. The $^{13}C$-labeled RNA CAAA-hairpin was prepared as described by Wijmenga et al. (1994a). The P(CC)H-TOCSY experiment was performed on a Bruker AMX(2)600 spectrometer, equipped with a broadband $^{13}C/^{1}H$ probe. The spectrum was recorded in approximately 12 h with the following acquisition settings: 512 scans for each FID of 1024 points ($t_2$), 64 $t_1$ values. The delay Δ was set to 25 ms; τ, τ' = 12.5 ms; 1 ms trim pulse; DIPSI3 mixing time for isotropic mixing equal to 13.0 ms and DIPSI3 mixing time for cross-polarisation set to 6.5 ms, both with an rf field strength of 8333.3 Hz, 1.0 s relaxation delay, 1 ms gradient pulse (800 μs gradient pulse shaped to a 1% truncated sine envelope and 200 μs for magnetic field recovery) of strength 12 G/cm, low-power GARP (Shaka et al., 1985) decoupling (rf strength 625 Hz) of $^{13}C$, spectral width 486 Hz, and 5000 Hz for $^{31}P$ and $^{1}H$, respectively; carrier positions at −2.09, 70 and 4.62 ppm for $^{31}P$, $^{13}C$ and $^{1}H$, respectively. Typical processing parameters were: zero-filling twice in $t_1$ and once in $t_2$, and 0.4 π shifted squared sine window multiplication in $t_1$ and $t_2$. The final data matrix consisted of 128 × 1024 data points.

the P(CC)H-TOCSY spectrum of the RNA hairpin (1.5 mM) in $D_2O$. The experiment is quite sensitive, since it could be recorded with good signal-to-noise ratio in approximately 12 h. An almost uninterrupted sequential walk can be made from the 5'-terminal residue G1 to the 3'-terminal residue U12. Interestingly, in Fig. 4 the connectivity between A8pG9 ($P_9$) is absent (although a very weak intensity at a lower threshold is visible). This can be attributed to two effects. First, the β torsion angle of G9 is shifted towards $g^-/g^+$, leading to a smaller value for the $J_{P5'C4'}$-coupling and thus decreasing the transfer efficiency via the C4'-route. In the 3D triple resonance HCP spectrum (Heus et al., 1994) this cross peak is present, although with lower intensity, so that the absence cannot be completely ascribed to this change in β. The second effect that contributes to the absence of this cross peak is the low intensity of the upfield shifted H1' resonance of G9. This resonance is broadened, probably due to conformational averaging; the H1'/C1' cross peak is also difficult to detect in an HMQC spectrum.

The P(CC)H experiment presented here bears some resemblance to the cross-polarisation approach by Kellogg and Schweitzer (1993). In the latter experiment the authors also attempted to obtain $^{31}P/^1H$ correlations in the H1' region of the spectrum to reduce resonance overlap. In the Kellogg experiments the transfer occurs via cross-polarisation from $^{31}P$ to $^1H3'$ and subsequently from H3' to H1', using either a longer cross-polarisation mixing time or a separate additional $^1H \rightarrow {}^1H$ isotropic mixing period. Because in this approach much smaller couplings are involved than in our approach, the transfer is much less efficient. Most significantly, for the transfer through the sugar ring we use the large $J_{CC}$-couplings (≈ 42 Hz), while in the approach of Kellogg the $J_{HH}$-couplings determine the transfer efficiency. In particular for RNAs it is virtually impossible to transfer magnetisation from H3' to H1', because of the small $J_{H1'H2'}$-couplings of ≈ 1 Hz for N-type sugars usually found in RNAs.

In summary, in this report we describe a simple and efficient 2D triple resonance NMR experiment which allows for unambiguous sequential backbone assignment of the H1' and $^{31}P$ resonances in $^{13}C$-labeled RNA oligonucleotides.

## Acknowledgements

This work was supported by the Netherlands Foundation for Chemical Research (SON) with financial aid from the Netherlands Organization for Advanced Research (NWO). We wish to thank J.W.M. van Os, J.W.G. Janssen and J.J. Joordens for excellent technical assistance. H.A.H. is supported by a grant from the Royal Netherlands Academy of Arts and Sciences.

## References

Batey, R.T., Inada, M., Kuyawinski, E., Puglisi, J.D. and Williamson, J.R. (1993) *Nucleic Acids Res.*, **20**, 4515–4523.

Bax, A. and Ikura, M. (1991) *J. Biomol. NMR*, **1**, 99–105.

Clore, G.M. and Gronenborn, A.M. (1990) *Annu. Rev. Biophys. Biophys. Chem.*, **20**, 29–63.

Clore, G.M. and Gronenborn, A.M. (1991) *Science*, **252**, 1390–1399.

Farmer II, B.T., Müller, L., Nikonowicz, E.P. and Pardi, A. (1993) *J. Am. Chem. Soc.*, **115**, 11040–11041.

Farmer II, B.T., Müller, L., Nikonowicz, E.P. and Pardi, A. (1994) *J. Biomol. NMR*, **4**, 129–133.

Grzesiek, S. and Bax, A. (1992) *J. Magn. Reson.*, **96**, 432–440.

Heus, H.A., Wijmenga, S.S., Van de Ven, F.J.M. and Hilbers, C.W. (1994) *J. Am. Chem. Soc.*, **116**, 4983–4984.

Ikura, M., Kay, L.E. and Bax, A. (1990) *Biochemistry*, **29**, 4659–4667.

Ikura, M., Kay, L.E. and Bax, A. (1991) *Biochemistry*, **30**, 5498–5504.

Kay, L.E., Ikura, M., Tschudin, R. and Bax, A. (1990) *J. Magn. Reson.*, **89**, 496–514.

Kay, L.E., Ikura, M. and Bax, A. (1991) *J. Magn. Reson.*, **91**, 84–87.

Kellogg, G.W. and Schweitzer, B.I. (1993) *J. Biomol. NMR*, **3**, 577–595.

Legault, P., Farmer II, B.T., Müller, L. and Pardi, A. (1994) *J. Am. Chem. Soc.*, **116**, 2203-2204.

Marino, J.P., Prestegard, J.H. and Crothers, D.M. (1994) *J. Am. Chem. Soc.*, **116**, 2205–2206.

Marion, D. and Wüthrich, K. (1983) *Biochem. Biophys. Res. Commun.*, **113**, 967–974.

Michnicka, M.J., Harper, J.W. and King, G.C. (1993) *Biochemistry*, **32**, 395–400.

Mooren, M.M.W., Hilbers, C.W., Van der Marel, G.A., Van Boom, J.H. and Wijmenga, S.S. (1991) *J. Magn. Reson.*, **94**, 101-111.

Nikonowicz, E.P. and Pardi, A. (1993) *J. Mol. Biol.*, **232**, 1141–1156.

Nikonowicz, E.P., Sirr, A., Legault, P., Jucker, F.M., Baer, L.M. and Pardi, A. (1992) *Nucleic Acids Res.*, **20**, 4507–4513.

Powers, R., Gronenborn, A.M., Clore, G.M. and Bax, A. (1991) *J. Magn. Reson.*, **94**, 209–213.

Shaka, A.J., Lee, C.J. and Pines, A. (1988) *J. Magn. Reson.*, **77**, 274–280.

Shaka, A.J., Barker, P.B. and Freeman, R.J. (1985) *J. Magn. Reson.*, **64**, 547–552.

Simon, E.S., Grabowski, S. and Whitesides, G.M. (1990) *J. Org. Chem.*, **55**, 1834–1847.

Sklenář, V., Peterson, R.D., Rejante, M.R., Wang, A. and Feigon, J. (1993a) *J. Am. Chem. Soc.*, **115**, 12181–12182.

Sklenář, V., Peterson, R.D., Rejante, M.R., Wang, A. and Feigon, J. (1993b) *J. Biomol. NMR*, **3**, 721–727.

Wijmenga, S.S., Mooren, M.M.W. and Hilbers, C.W. (1993) In *NMR of Macromolecules* (Ed., Roberts, G.C.K.) Oxford University Press, Oxford, pp. 217–288.

Wijmenga, S.S., Heus, H.A., Van de Ven, F.J.M. and Hilbers, C.W. (1994a) In *NMR of Biological Macromolecules* (Ed., Stassinopoulou, C.I.) NATO ASI Series, Vol. 87, Springer, Berlin, pp. 307–322.

Wijmenga, S.S., Hoppe, H., Van der Graaf, M., Heus, H.A. and Hilbers, C.W. (1994b) manuscript in preparation.

Wijmenga, S.S., Heus, H.A., Werten, B.A., Van der Marel, G.A., Van Boom, J.H. and Hilbers, C.W. (1994c) *J. Magn. Reson. Ser. B*, **103**, 134–141.

Wüthrich, K. (1986) *NMR of Proteins and Nucleic Acids*, Wiley, New York, NY.

Zuiderweg, E.R.P. (1990) *J. Magn. Reson.*, **89**, 533–542.